Effects of Mutations of the Bulged Nucleotide in the Conserved P7 Pairing Element of the Phage T4 *td* Intron on Ribozyme Function†

Renée Schroeder,‡,§ Uwe von Ahsen,§ and Marlene Belfort*,‡,∥

Wadsworth Center for Laboratories and Research, New York State Department of Health, Empire State Plaza, P.O. Box 509, Albany, New York 12201, School of Public Health, State University of New York at Albany, Empire State Plaza, Albany, New York 12201, and Institut für Mikrobiologie und Genetik der Universität Wien, Althanstrasse 14, 1090 Vienna, Austria

Received August 31, 1990; Revised Manuscript Received December 6, 1990

ABSTRACT: The P7 element of group I introns contains a semiconserved "bulged" nucleotide, a C in group IA introns (nt 870 in the *td* intron) and an A in group IB introns [Cech, T. R. (1988) *Gene 73*, 259–271]. Variants U870, G870, and A870, isolated by a combination of in vitro and in vivo genetic strategies, indicate that C and A at position 870 are consistent with splicing whereas U and G are not. Although mutants G870 and U870 could be activated in vitro by increasing the Mg^{2+} concentration, their K_m for GTP at pH 7 was 20–100-fold elevated, and they were unable to undergo site-specific hydrolysis. The dependence of the mutants on high guanosine concentrations could be substantially overcome by an increase in pH, suggesting that a tautomeric change, which makes U and G mimic C and A, is responsible for restoring function. In contrast to the striking K_m effect, V_{max} for the mutants differed by less than a factor of 2 from the wild type. Furthermore, streptomycin, an aminoglycoside antibiotic that competes with guanosine for its binding site, inhibited splicing of the U870 and G870 constructs at least as well as of the C870 and A870 variants, indicating that the guanosine-binding site of the mutants is proficient at interacting with a guanidino group. While our experiments argue against a hydrogen-bonding interaction between the C_6–O of the cofactor and C_4–NH_2 of the bulged nucleotide, they are consistent with other models in which the C_4–NH_2 and/or N_3 groups of the bulged C are involved in establishing an active ribozyme.

Group I introns fold into a very distinctive structure to form a catalytically active RNA molecule (Figure 1A). The extensive secondary structure, which includes pairing elements P1–P10 (Michel et al., 1982; Davies et al., 1982; Burke et al., 1987), has been proposed to involve tertiary interactions that result in formation of two large coaxially stacked helices (Kim & Cech, 1987; Michel & Westhof, 1990). The excision of the intron is a two-step reaction [reviewed by Cech (1987, 1990)]. First, guanosine binds to the guanosine-binding site (G-site) (Michel et al., 1989), and the cleavage of the 5′ splice site occurs in a transesterification reaction, during which guanosine is covalently linked to the first nucleotide of the intron. In a second transesterification reaction, after the last nucleotide of the intron (always a G) is brought into the G-site, the 3′ splice site is cleaved, and the exons are ligated.

The guanosine cofactor is proposed to associate with the ribozyme via its guanidino, keto, and ribose OH groups (Bass & Cech 1984, 1986; Figure 2). Interaction with two donor groups of guanine has been shown to occur via the G of a conserved G-C pair in P7 of the *Tetrahymena* intron (G264). G264 also appears responsible for binding the terminal G of the intron, suggesting that one binding site is involved in guanosine binding for 5′ splice site cleavage and for exon ligation (Michel et al., 1989). Two binding sites have, however, been proposed for the guanosine exchange reaction (Kay et al., 1988).

Bulged nucleotides are common elements of RNA secondary structure and are known to be involved in the function of many RNA molecules. First, in the splicing of group II introns and in the spliceosome-dependent splicing of nuclear pre-mRNAs in yeast, it is the bulged nucleotide of a critical pairing that forms the 2′–5′ linkage of the lariat (Parker et al., 1987; Peebles et al., 1986). Second, bulged nucleotides appear in 12 locations in the current *Escherichia coli* 16S RNA secondary structure (Noller et al., 1985). Some of these, as well as the bulged residues in the R17 RNA phage operator and HIV-1 TAR RNA, have been associated with the binding of proteins (Christiansen et al., 1985; Wu & Uhlenbeck, 1987; Roy et al., 1990). Bulged nucleotides have also recently been suggested to facilitate conformational transitions in double-stranded RNA helices (White & Draper, 1989).

We therefore turned our attention to unpaired nucleotides of the *td* intron that might have particular functional significance. Our selection of residues for study was based on two collections of nondirected splicing-defective mutants, isolated on the basis of reduced production of the *td* product thymidylate synthase (TS) (Hall et al., 1987; Belfort et al., 1987; Chandry & Belfort, 1987; Ehrenman et al., 1989). Most mutations (among more than 30 independent isolates) disrupt double-stranded RNA regions in the predicted secondary structure (Figure 1A), whereas 5 mutations are in apparently unpaired residues (Figure 1A). We selected the semiconserved bulged nucleotide (C870) in the highly conserved P7 element of the catalytic core of the *td* intron for further study. Since the initiation of this work, the nucleotide immediately 3′ to the equivalent bulged residue in the *Tetrahymena* intron was shown to be part of the G-site (G264) that binds the guanine

† This work was supported by NSF Grant DMB8502961 and NIH Grants GM39422 and GM44844 to M.B. and by Fonds zur Förderung der wissenschaftlichen Forschung, Vienna, Austria, to R.S.

* Author to whom correspondence should be addressed at Wadsworth Center for Laboratories and Research, New York State Department of Health.

‡ New York State Department of Health.

§ Institut für Mikrobiologie und Genetik der Universität Wien.

∥ State University of New York at Albany.

0006-2960/91/0430-3295$02.50/0

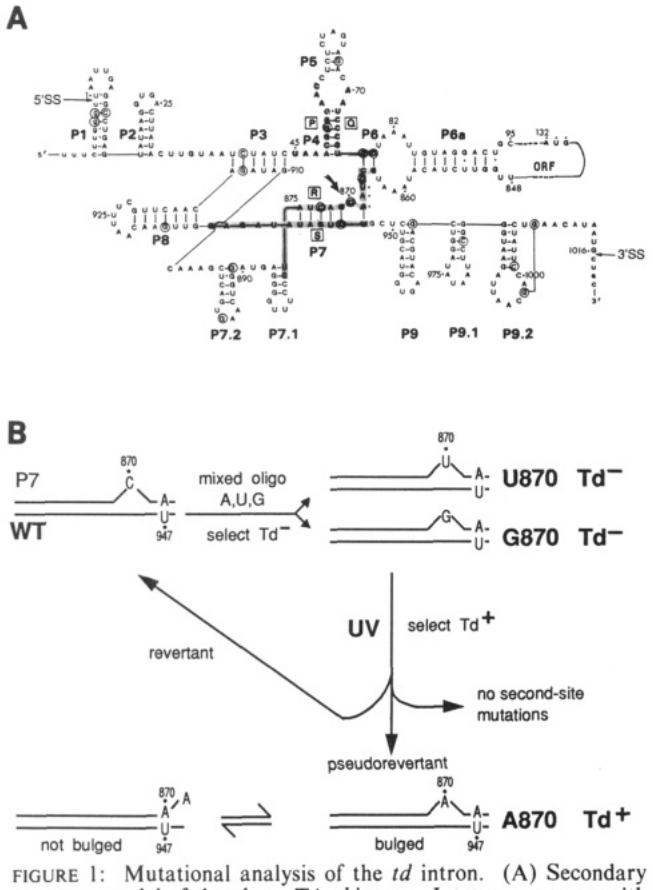

FIGURE 1: Mutational analysis of the *td* intron. (A) Secondary structure model of the phage T4 *td* intron. Intron sequences, with pairing elements P1–P9.2, are in upper case letters and exon sequences in lower case letters. Conserved sequence elements P, Q, R, and S are shaded. Small numbers indicate intron residues. Mutations causing splicing defects are circled (21 residues, representing the location of 31 independent isolates). The bulged nucleotide in P7 is indicated with a heavy arrow. (B) Schematic for site-directed mutagenesis and reversion analysis. WT = wild type (C870). The scheme for isolating mutants (U870, G870) and the pseudorevertant (A870) is described in the text. The paired and unpaired states of A870 are shown at the bottom of the figure.

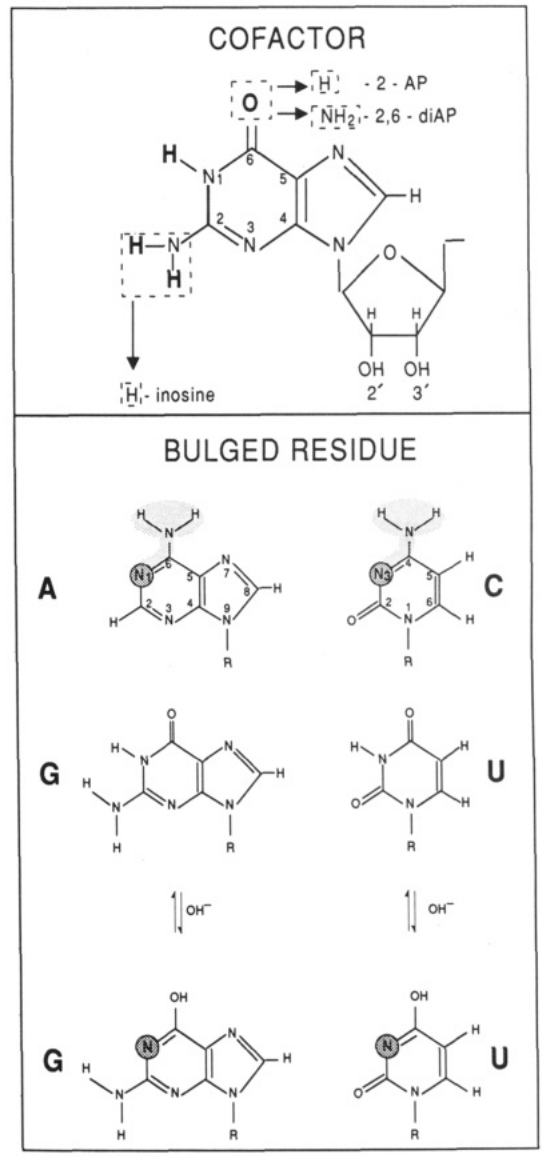

FIGURE 2: Guanosine cofactor is shown in the upper panel. The atoms proposed to be involved in H-bonding to the ribozyme are boldface (Bass & Cech, 1984). Bonds between N_1–H and one of the H's of C_2–NH_2 to C_6–O and N7, respectively, of G264 of the *Tetrahymena* intron have been experimentally verified (Michel et al., 1989). Altered substituents in the analogues 2-aminopurine (2-AP), 2,6-diaminopurine (2,6-diAP), and inosine are indicated. The bulged residue is depicted in the lower panel. The similar charge density distribution of C and A around C_4–NH_2/N_3 and C_6–NH_2/N_1, respectively, is indicated by shading. G and U may undergo tautomeric changes at alkaline pH, so that their charge distribution then more closely resembles that of A and C at positions N_1/C_6 and N_3/C_4 (relevant N's circled), respectively (Saenger, 1984).

moiety of the cofactor (Michel et al., 1989).

The semiconserved bulged nucleotide in P7 is a C in group IA introns and an A in group IB introns (Cech, 1988). We changed this bulged C of the group IA *td* intron to A, U, and G by a combination of site-directed and nondirected mutagenesis. Subsequently, function of the four constructs (C870, A870, U870, and G870) was compared both in vivo and in vitro to learn more about the role of this residue in splicing and hydrolysis.

Materials and Methods

Bacterial Strains and Plasmids. *E. coli* strain JM109*thy*A is a *thy*A derivative isolated in this laboratory from JM109 and was used as the host strain for all in vivo experiments. Strain CJ236 (*dut*, *ung*, *thi*-1, *rec*A, *spo*T1, F′, Cam^R) was used to isolate uridine-containing DNA (Vieira et al., 1987). M13 helper phage KO7 (Km^R) was used to isolate single-stranded DNA.

The parental *td* construct pTZ18U-ΔP6-2 containing a 751-nucleotide deletion in the L6a region has a 265-nt intron with full splicing activity (Salvo et al., 1990). For some experiments, constructs with truncated exons were used. Plasmid pTZ18U-ΔP6-2 and the three constructs derived therefrom (U870, G870, and A870) were digested with *Nde*I and the 5′ extensions filled using T4 DNA polymerase. The 365-nt fragment containing the intron, 79 nt of exon I and 21 nt of exon II, was gel-purified and cloned into the *Sma*I site of pTZ18U. The two families of constructs are referred to as the L (long) and T (truncated) constructs, respectively. The former were used primarily to detect in vivo phenotypes whereas the latter were used for most in vitro experiments, as indicated.

Media and Growth Conditions. Growth medium was TBYET, tryptone broth (1% Bactotryptone and 0.5% NaCl) supplemented with 0.5% yeast extract and 50 μg/mL thymine. Minimal medium supplemented with casamino acids (Belfort et al., 1983) but lacking thymine (–THY medium) was used to select for the Td^+ (TS^+) phenotype. TTM, a minimal medium supplemented with thymine (50 μg/mL) and trimethoprim (20 μg/mL), was used to screen for the Td^- (TS^-)

phenotype, as only cells lacking TS activity are able to grow on media containing the folate analogue trimethoprim. Unless otherwise indicated, the cells were grown at 37 °C.

Oligonucleotide-Directed Mutagenesis. A mixed oligonucleotide (5′-GGATAGTCXTTAGGCAT-3′, where X = A, T, or C) was used. Deoxyuridine-substituted single-stranded DNA was isolated following the procedure of Kunkel et al. (1987) and Vieira et al. (1987). Annealing of the phosphorylated oligonucleotide to single-stranded DNA, elongation, and ligation were according to Williamson et al. (1989). After transformation, the colonies were screened on TTM for the Td^- phenotype. The mutations were identified by dideoxy sequencing of double-stranded DNA (Bartlett et al., 1986).

Reversion Analysis. Constructs obtained after site-directed mutagenesis (U870 and G870) were used for nondirected mutagenesis. Cells (2×10^8) from a fresh overnight culture were spread on a −THY plate, irradiated with a UV germicidal lamp (254 nm, 0.16 A; from Ultra Violet Products Inc., Model UVG-54) from a distance of 21 cm for 10 s to yield 50% survivors. The plates were then incubated at 37 °C for 2 days. Plasmids were extracted from colonies that grew (TS^+) and used to retransform *thy*A (TS^-) cells, to verify that the TS^+ phenotype was a property of the *td* gene. The Td^+ revertants were then sequenced (Figure 1B).

RNA Slot-Blot Assay. RNA was extracted from cells that had been grown to OD_{650} 0.2 and induced with 2 mM isopropyl β-D-thiogalactoside (IPTG) for 1 h. One microgram of total RNA was transferred to a nylon filter and hybridized with ^{32}P end-labeled oligonucleotide complementary to exon I (5′-GGTCTACACCACCAAAATC-3′) or to the splice junction (5′-ATTAAACGGTAGACCCAAGAAAAC-3′) (Hall et al., 1987). Autoradiographs were quantitated by densitometry of film that had been exposed in the linear range.

In Vitro Transcription and Pre-mRNA Isolation. DNA was prepared by the alkaline-lysis procedure and linearized with *Eco*RV (the L constructs) or *Hin*dIII (the T constructs). Transcription was in a total volume of 25 μL at 30 °C for 1 h in buffer containing 40 mM Tris-HCl, pH 7.5, 3 mM $MgCl_2$, 0.4 mM spermidine, a 1 mM aliquot of each of the rNTPs, 5 mM DTT, 10 units of T7 RNA polymerase (Stratagene), 10 μCi of [α-^{35}S]CTP, and 10 units of RNase block (Promega). The reaction was stopped on ice by adding 200 μL of stop solution (0.1 mg/mL yeast tRNA/2.5 mM EDTA), 100 μL of 7.5 M NH_4OAc, and 750 μL of ethanol. The precipitate was resuspended in 20 μL of diethyl pyrocarbonate treated H_2O and loaded on a 5% acrylamide/7 M urea gel. Bands were cut out of the gel and soaked in 300 μL of elution buffer (10 mM Tris-HCl, pH 7.5, 10 mM EDTA, and 3.5 M NH_4OAc) for several hours at 37 °C. After centrifugation, the supernatant was ethanol-precipitated. The pre-mRNA was then resuspended in H_2O at 30 000 cpm/μL. All splicing assays except those in Figure 4 were performed on gel-purified pre-mRNA that had been reactivated according to Walstrum and Uhlenbeck (1990).

In Vitro Splicing and Hydrolysis Assays. For determination of the GTP requirement (Figure 5A–D), pre-mRNA (30 000 cpm) was incubated for 10 min at 37 °C in a total volume of 5 μL of buffer containing 40 mM Tris-HCl, pH 7, 8 mM $MgCl_2$, and 0.4 mM spermidine with increasing amounts of GTP (0–100 μM). The reactions were stopped by adding 5 μL of FDM (0.01% bromophenol blue and 0.01% xylene cyanol in formamide) and run on 5% acrylamide/7 M urea gels. For determination of the K_m for GTP (Figure 5E), precursor was incubated with four different amounts of GTP for 0, 1, 5, 10, and 30 min. Autoradiograms were scanned and integrated with a Hoeffer densitometer using the GS365 program. The extent of reaction at a given time was calculated by summing the reaction products (exon I + intron–exon II + intron + ligated exons), and the initial velocity was determined from the slope of the time course plots. Each measurement was repeated twice. K_m determinations for the guanosine analogues were similar, except that experiments were performed at higher relative substrate–analogue concentrations. Hydrolysis was assayed at 42 °C for 15 min in buffer containing 40 mM Tris-HCl, pH 9, 0.4 mM spermidine, and 8 mM $MgCl_2$. For determination of the rate of the reaction per minute, pre-mRNA was incubated under the same conditions as for determination of the guanosine requirement, except that the GTP concentration was 500 μM. Incubation times were 0, 0.5, 1, 2, 5, 10, and 30 min. Autoradiographs were processed as for K_m determination. Each measurement was repeated 4 times.

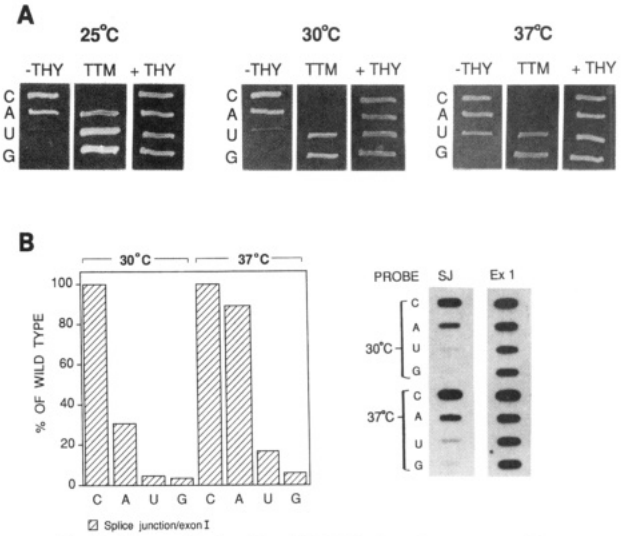

FIGURE 3: In vivo analysis. (Panel A) Plating phenotypes. Constructs were plated on selective media: −THY = minimal medium lacking thymine, TTM = minimal medium supplemented with thymine and trimethoprim, +THY = nonselective complete medium. C = wild type C870, A = pseudorevertant A870, U = mutant U870, and G = mutant G870. (Panel B) RNA analysis. The slot blot on the right shows total RNA, extracted from IPTG-induced cells, bound to nylon, and hybridized to oligonucleotides complementary to the splice junction (SJ) and to exon I (Ex 1). Quantitation of autoradiograph scans is represented on the left. Values were normalized by dividing splice–junction signals by exon I signals and expressed relative to C870 (100%).

RESULTS

Site-Directed Mutagenesis and Reversion Analysis. The *td* construct pTZ18U-ΔP6-2, here referred to as C870, or wild type, was mutagenized by using a mixed oligonucleotide so that the RNA would have a G, an A, or a U at the position corresponding to residue 870 (Figure 1A,B). The transformants were screened after mutagenesis for splicing defects by their ability to grow on TTM-containing plates (see Materials and Methods). Thereby, mutants U870 and G870 were obtained. Subsequently, constructs U870 and G870 were screened in vivo for revertants able to grow on thymine-less media. TS^+ pseudorevertant A870 and true revertant C870 were isolated repeatedly, both spontaneously and after UV mutagenesis, but no second-site compensatory mutant that mapped within the intron could be found (Figure 1B). Although these results suggest that C870 is not involved in a long-range pairing, we cannot eliminate the possibility that a pairing partner may be bifunctional, and a mutation would

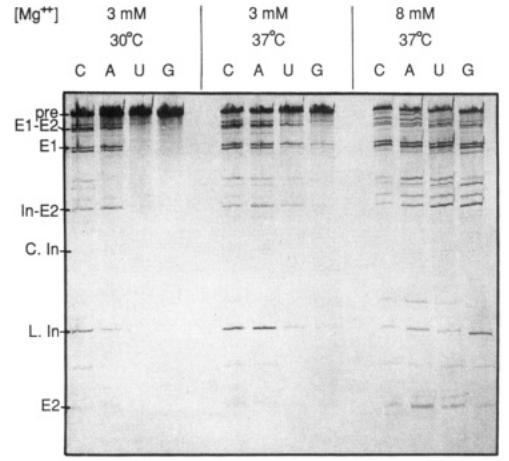

FIGURE 4: Condition dependence of splicing. Linearized templates of the four L constructs (C870, A870, U870, and G870) were transcribed in vitro under three different conditions of temperature and Mg^{2+} concentration, as indicated. Samples were separated on 5% acrylamide/7 M urea gels. RNA species and their sizes are as folows: pre = pre-mRNA, 1241 nt; E1–E2 = ligated exons, 976 nt; E1 = free exon I, 774 nt; In–E2 = intron–exon II, 468 nt; C.In = circular intron, 264, nt; L.In = linear intron, 266 nt; E2 = free exon II, 202 nt. Doublets corresponding to E1 and E1–E2 reflect the use of a cryptic 5′ splice site in exon I (Chandry & Belfort, 1987). Other bands appearing at 8 mM Mg^{2+} have not been identified.

then lead to an inactive intron.

In Vivo Phenotypes. The in vivo TS phenotype of the four constructs was tested by plating them on selective media (Figure 3A). The constructs U870 and G870 did not grow appreciably on thymine-less media at 25 or 30 °C whereas both grew on TTM medium, indicating that they are severely defective in TS production. Although construct G870 did not grow on thymine-less media at any temperature, U870 was able to grow somewhat in the absence of thymine at 37 °C. However, U870 also grew on TTM, suggesting that at this temperature the defect of this mutant was only partially restored. In contrast, the pseudorevertant A870 grew very well on media lacking thymine at all three temperatures tested (25, 30, and 37 °C) and grew on TTM only at 25 °C, indicating that the restoration of TS production is very efficient, albeit not complete.

To quantify the splicing ability of the four constructs in vivo, RNA was extracted from cells grown at 30 and 37 °C. Equal amounts of RNA were bound to a nylon filter and hybridized to oligonucleotides complementary to exon I and to the splice junction. Results shown in Figure 3B agree well with the TS plating phenotypes. Construct A870 accumulated 89% of the wild-type amount of mRNA at 37 °C, whereas constructs U870 and G870 had only 16% and 6% of the wild-type levels, respectively. Furthermore, a temperature dependence is suggested by the observation that at 30 °C the amounts of mRNA relative to wild type were 30% for A870 and ca. 4% for U870 and G870.

Magnesium Restores Splicing Activity in Vitro. The mutants were further analyzed in vitro. First, plasmid DNA of the four L constructs (with full-length exons), linearized in exon II, was transcribed under different conditions of buffer and temperature, with 3 mM Mg^{2+} best mimicking their in vivo phenotypes (Figure 4). At low Mg^{2+} concentration at 30 °C, only the wild type C870 and the pseudorevertant A870 were able to splice, whereas at 37 °C mutant U870 was slightly more active (see appearance of E1–E2), indicating that the temperature dependence extends to the in vitro situation. Raising the Mg^{2+} concentration to 8 mM at 37 °C activated mutants U870 and G870 to wild-type levels of splicing. All following in vitro assays were therefore performed at 8 mM $MgCl_2$. This enabled the analysis of distinctive splicing activities of the two mutants U870 and G870. These latter experiments were conducted at pH 7.0, except where indicated, to cut down on the multiplicity of products seen at pH 7.5 in Figure 4.

Table I: Splicing Parameters Determined for the Bulged Nucleotide Variants

construct	K_m (μM)[a] T	L	V_{max}[b] (min^{-1})	initial velocity[c] (min^{-1})	In–E2/ E1–E2[d]
C870	0.8	1	0.40	0.20	0.8 ± 0.2
A870	4	2	0.33	0.17	1.0 ± 0.2
U870	75	100	0.63	0.16	1.7 ± 0.4
G870	25	20	0.38	0.28	2.2 ± 0.4

[a] K_m values for GTP for the truncated constructs (T) are from Figure 5E. Data for the long (L) constructs are not shown. [b] V_{max} was determined from the data in Figure 5E. [c] The amount of product accumulated in 1 min is expressed relative to the total amount of product produced (30 min) at a GTP concentration of 500 μM. [d] The ratios of intron–exon II (In–E2) to ligated exons (E1–E2) are average values ascertained from time course experiments at the same GTP concentrations used for K_m and V_{max} determinations. The ratios have been corrected for the relative cytosine content of the two species.

K_m and V_{max} Determinations. Gel-purified, reactivated pre-mRNA of the four T constructs (with truncated exons) was incubated with increasing amounts of GTP for 10 min at 37 °C (Figure 5A–D). A pH of 7 was shown to be optimal for supporting splicing versus site-specific hydrolysis for the wild type (Figure 6A). For determination of the K_m for GTP and V_{max}, pre-mRNA of the four T constructs was incubated at four different GTP concentrations (selected on the basis of the data in Figure 5A–D) for increasing times. K_m values derived from the data in Figure 5E are summarized in Table I along with K_m values from an independent experiment with the L constructs. Thus, the K_m for GTP was found to be ~1 μM for the wild type C870 [in good agreement with that determined independently for the *td*Δ1-3 construct (Hicke et al., 1989)], 2–4 μM for the pseudorevertant A870, 20–25 μM for the mutant G870, and 75–100 μM for the mutant U870.

In contrast to these differences of up to 100-fold in K_m, V_{max} varied by less than a factor of 2 from wild type, as did the amount of product formed in the first minute of the reaction at saturating GTP concentrations (Table I). The overall extent and accuracy of splicing (i.e., exon ligation) were also similar in the mutants at elevated Mg^{2+} and GTP concentrations (Figures 4 and 5 and data not shown). Furthermore, under these conditions, activity at the 3′ splice site appeared to be only modestly affected. This conclusion is based on the ratio of the product of the first step of splicing (intron–exon II) to that of the second step (ligated exons), which varied by less than a factor of 3 in the mutants (Table I). It is noteworthy that the exon ligation step for the *td* intron appears less efficient than for the *Tetrahymena* intron, which rarely accumulates the intron–exon II intermediate. This difference may be attributed to the P9.0 and P10 pairings, which anchor the 3′ splice site for exon ligation, and which are very weak in the case of the *td* intron (Michel et al., 1989, 1990; Burke et al., 1990).

GTP Requirement Is Lower at pH 9. The requirement for GTP for the mutants U870 and G870 was further determined at pH 9. By shifting the pH from 7 to 9, the requirement for GTP of the two mutants U870 and G870 dropped (Figure 5C,D), suggesting that the mutated ribozymes have a higher affinity for the guanosine cofactor at pH 9. Although these experiments could not be performed with the wild type and the pseudorevertant, because of strong site-specific hydrolysis

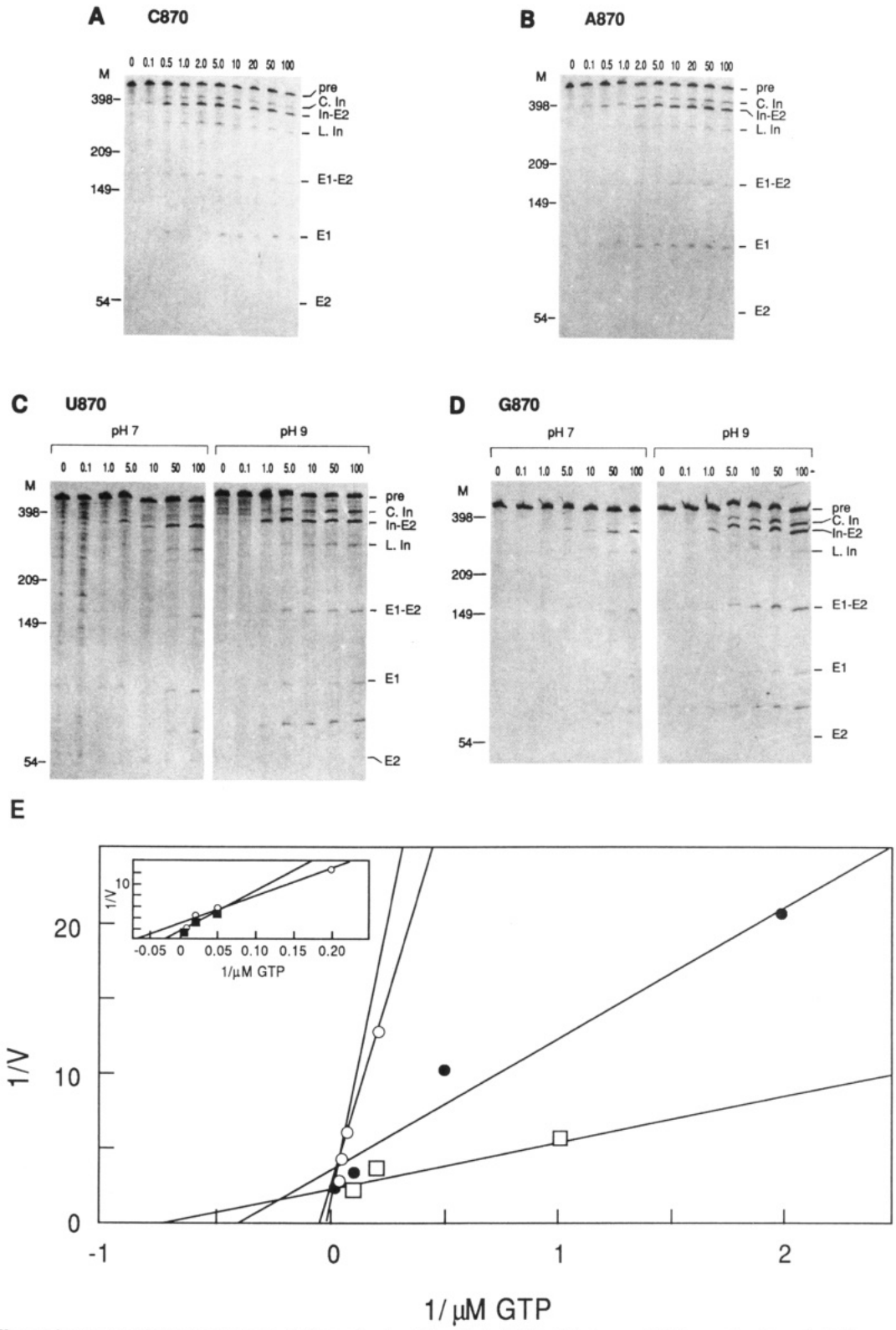

FIGURE 5: GTP requirement and pH dependence of T constructs. (Panels A–D) Purified pre-mRNA was incubated with increasing amounts of GTP for 10 min at pH 7, unless otherwise indicated. The GTP concentration is shown above each lane in micromolar. The sizes in nucleotides of RNA markers are indicated to the left of each autoradiogram (M). RNA species indicated on the right of each autoradiogram are labeled as in Figure 4. (Panel E) A Lineweaver–Burk plot is shown for the bulged nucleotide variants, where initial velocities were determined at different GTP concentrations (see Materials and Methods). (□) C870; (●) A870; (■) U870; (○) G870. The inset shows the high-K_m mutants, for which some points are obscured in the larger graph. For wild type, a fourth point, at low GTP concentration, was used to determine the line plot. This point falls outside of the graph shown.

at pH 9 (Figure 6), we measured the GTP dependence of the wild-type ribozyme between pH 7.0 and 7.8. While splicing was more efficient at higher pH, no reduction in GTP requirement was seen (data not shown). These results indicate that the observed pH-dependent decrease in the substrate requirement is specific for the mutants.

Mutants U870 and G870 Do Not Undergo Site-Specific Hydrolysis. Some phosphodiester bonds in the ribozyme are particularly sensitive to nucleophilic attack and undergo hydrolysis with increasing pH. These are bonds at the 5′ and

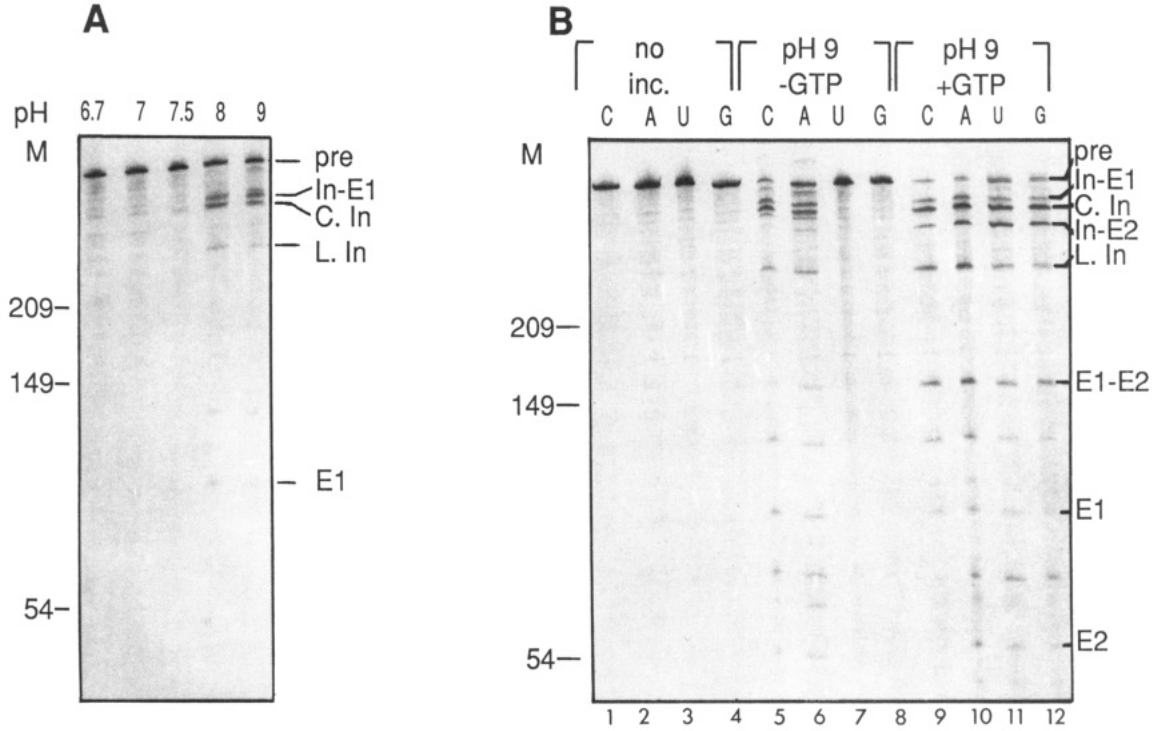

FIGURE 6: Site-specific hydrolysis with T constructs. (Panel A) pH dependence. Purified pre-mRNA of the wild type C870 was incubated in buffers of increasing pH as indicated above the lanes. Note the appearance of In–E1, a major hydrolysis product, with increasing pH. It is likely that C.In, results from attack of the 3′-G of the intron at the 5′ splice site and that L.In results from circle reopening (Inoue et al., 1986). (Panel B) Pre-mRNA of the four constructs (C870, A870, U870, and G870, lanes 1–4) was incubated in Tris-HCl, pH 9, without GTP (lanes 5–8) or with 100 μM GTP (lanes 9–12). Markers (M) and RNAs are labeled as in Figure 5.

3′ splice sites and at the intron cyclization junction (Zaug et al., 1984, 1985; Cech, 1987). Products corresponding to hydrolysis at these sites appeared when the wild type (C870) and pseudorevertant (A870) were incubated in the absence of GTP at increasing pH (Figure 6A,B). In contrast, constructs U870 and G870 did not undergo hydrolysis, and their pre-mRNAs were stable even at pH 9 in the absence of guanosine (42 °C and 8 mM Mg^{2+}). As previously indicated, hydrolysis of the wild type and of the pseudorevertant were pH-dependent, and could be minimized at pH 7 (Figure 6A). Although the GTP requirement was much lower at pH 9, the mutants were not able to undergo site-specific hydrolysis at this pH. These results suggest that water, which attacks the labile phosphodiester bonds in the absence of guanosine, cannot act as a nucleophile in the mutants.

Interaction of the C870 Variants with Guanosine Analogues. To address whether the substrate guanosine undergoes a hydrogen bond with the bulged nucleotide in P7, we analyzed guanosine analogues as splicing cofactors. Bass and Cech (1984, 1986) argued that guanosine is likely to undergo four hydrogen bonds with the ribozyme, in addition to interactions with the ribose moiety. There are thought to be two hydrogen bonds with the amino group C_2–NH_2, one with the keto group C_6–O, and one with N_1–H (Figure 2). For the *td* intron, cofactor positions N_1–H and C_2–NH_2 are likely to form two H-bonds to C_6–O and N7 of G871, respectively, by analogy with cofactor interactions with G264 of the *Tetrahymena* intron (Michel et al., 1989). To probe other possible interactions, inosine (lacking C_2–NH_2), 2-aminopurine (lacking C_6–O), and 2,6–diaminopurine (with an NH_2 group replacing C_6–O) were used as guanosine analogues. Both mutants U870 and G870 showed increased requirements for all these cofactors when compared to the wild type and to the pseudorevertant, indicating that none of these analogues could compensate for the defect. Sample data are shown for 2,6-diaminopurine in Figure 7, where the analogue supports splicing of C870 and A870 at 30 μM but not of U870 and G870 even at 300 μM. The K_m for 2,6-diaminopurine with the wild type C870 was ca. 100 μM and >3 mM with mutant U870.

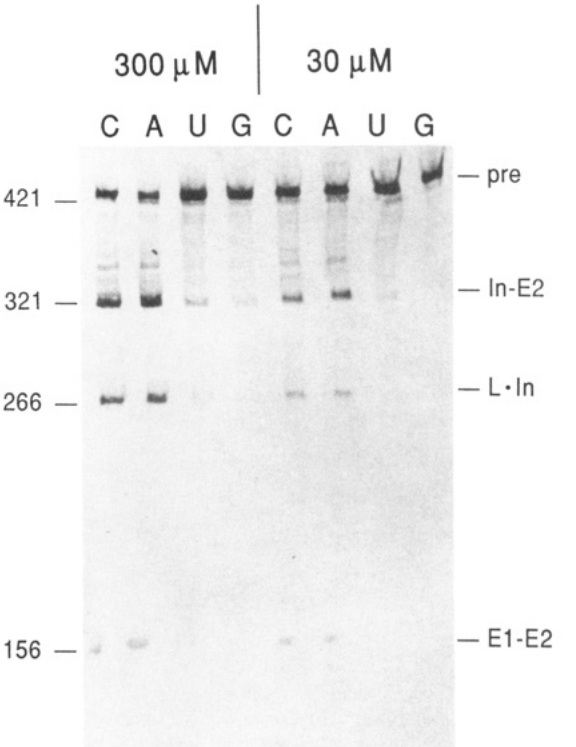

FIGURE 7: Splicing with the cofactor 2,6-diaminopurine. Pre-mRNA of the four N870 variants was incubated in the presence of 30 or 300 μM 2,6-diaminopurine at pH 7, in the absence of guanosine for 10 min under otherwise similar experimental conditions to those described for Figure 5.

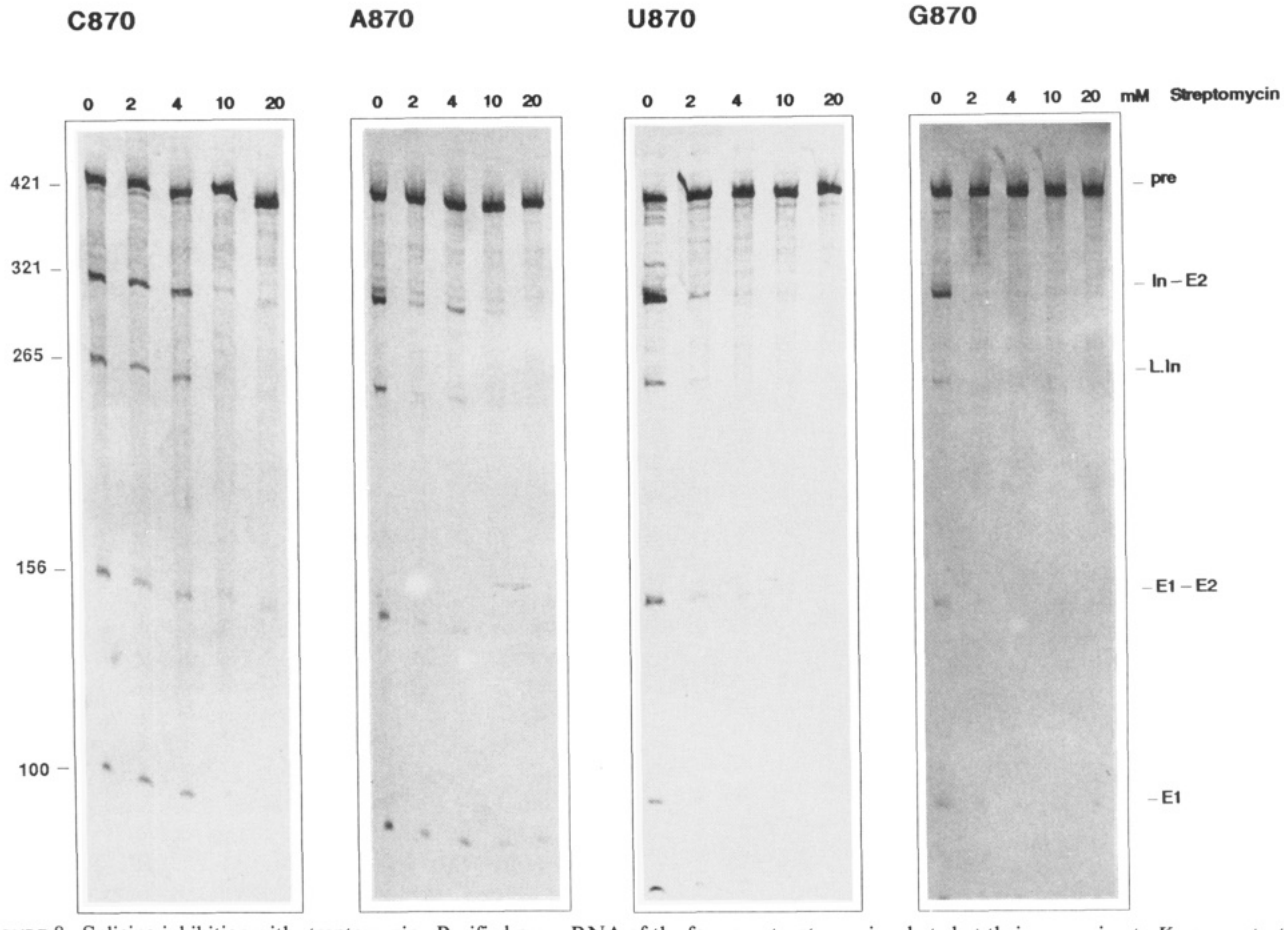

FIGURE 8: Splicing inhibition with streptomycin. Purified pre-mRNA of the four constructs was incubated at their approximate K_m concentration for GTP (1, 2, 100, and 20 μM for C870, A870, U870, and G870, respectively) with the indicated concentrations of streptomycin. Incubation was for 10 min at pH 7 as for Figure 5. RNAs are labeled as in Figure 5.

Furthermore, the K_m for inosine with C870 was ca. 300 μM and >6 mM for U870. Although these results do not suggest any unexpected interactions, the 2,6-diaminopurine data argue against hydrogen-bond formation between the keto group of the cofactor and the amino group of the bulged nucleotide (see Discussion).

In analogy to arginine, which competes with guanosine for the binding site via its guanidino group (Yarus, 1988), streptomycin, an aminoglycoside antibiotic that contains two guanidino groups, is able to inhibit splicing by competition with guanosine (von Ahsen & Schroeder, 1990). We therefore wished to determine the effect of streptomycin on the bulged nucleotide mutants. Incubation of the four variants with increasing amounts of streptomycin and GTP at the respective K_m concentrations for each of the variants inhibited splicing in all four cases (Figure 8). While there was a slight increase in binding affinity for streptomycin (K_I was 2–5-fold depressed for the mutants), the inhibition was relieved in all cases by the addition of guanosine to the reaction (R. Schroeder and U. von Ahsen, unpublished results). This indicates that the G-site in the mutated ribozymes (U870 and G870) is capable of binding the guanidino group and that the bulged residue does not interact with this group. Streptomycin sensitivity also argues against massive distortion of the G-site.

Discussion

Conserved and semiconserved residues that are in apparently unpaired regions of the group I intron core structure are of particular interest with respect to their functional contribution to the ribozyme. A mutational analysis of the bulged nucleotide in the highly conserved P7 element of the *td* intron (C870) was therefore undertaken to study the role of this residue in splicing. Both in vivo (Figure 3) and in vitro studies (Figures 4–8) indicated that whereas U and G at position 870 result in a dramatic reduction in splicing activity, an A at this site is consistent with function. The functional interchangeability of C and A is corroborated by phylogenetic data, with the bulged residue in nature being either C or A and never U or G (Cech, 1988; Michel & Westhof, 1990).

Interestingly, unlike the wild type C870, A870 has the option to pair with nucleotide U947 and not to bulge at all (Figure 1B). In contrast, where group IB introns naturally contain a bulged A in P7, the last nucleotide in P7 (conserved sequence element S), corresponding to nucleotide U947 of the *td* intron, is a C, assuring maintenance of the bulged structure (Cech, 1988; Couture et al., 1990). The bulged versus paired structural alternatives available to the A870 variant may account for the temperature-dependent reduction in splicing activity of this pseudorevertant in vivo (Figure 3) and for a slightly elevated K_m for GTP (Figure 5, Table I). With respect to other in vitro properties, the A870 constructs deviate little from the wild type (Figures 4–8), suggesting that the A870 variant has the propensity to stay bulged, possibly by interacting with another nucleotide, as has recently been proposed by Michel and Westhof (1991). On the basis of three-dimensional modeling, these authors have predicted an interaction between the amino group of the bulged nucleotide (C_6–NH_2 of A or C_4–NH_2 of C) with the phosphate 5' to a conserved A residue located 2 nt upstream (A261 of the *Tetrahymena* intron and A868 of the *td* intron, in J6/7, the junction between P6 and P7).

Couture et al. (1990) have measured the activity of bulged

nucleotide variants in the group IB *Tetrahymena* rRNA intron. Although their results also indicate the compatibility of either A or C with function, the activity of both A and C variants dropped sharply when these residues were able to base-pair with their complement in the 3' element of P7. This difference between the two introns may be attributable to the use of a modified *Tetrahymena* intron, which is particularly sensitive to mutation (Couture et al., 1990).

The phenotypes of the variants U870 and G870 may be summarized as follows: The mutants need higher amounts of Mg^{2+} and of the cofactor guanosine to splice (20–100-fold increase in K_m for GTP), and they do not undergo site-specific hydrolysis. In contrast, the V_{max} as well as the initial velocity of the reaction at high Mg^{2+} and GTP concentrations is minimally affected. Furthermore, the increased requirement for guanosine can be partially overcome by increasing the pH. In rationalizing these phenotypes, together with the response of the mutants to guanosine analogues, three options are considered below for the function of the bulged residue: H-bonding with the purine ring of the cofactor, activation or positioning of the nucleophile for attack at the 5′ splice site, and structural contribution to the G-site.

First, the similar charge density distribution around C_4–NH_2 and N_3 of C and C_6–NH_2 and N_1 of A (Figure 2) prompts speculation on their interaction with the cofactor. Although our experiments do not address an interaction with the ring nitrogen N3, they argue against an H-bond involving C_4–NH_2. Specifically, the inability of 2,6-diaminopurine to relieve the phenotype of the U870 mutant (Figure 7), with which it should produce a compensatory H-bond (Michel et al., 1989), argues against interaction of the C_6–O group of the cofactor with C_4–NH_2 of C870 (Figure 2).

Second, a function for the bulged nucleotide in facilitating nucleophilic attack at the 5′ splice site by the ribose 3′-OH is consistent with the phenotypic properties of the mutants. Michel and Westhof (1990) have proposed that in addition to the conserved A (A868) in J6/7 interacting with the amino group of the bulged nucleotide, this A also interacts with the ribose 2′-OH of the cofactor or of the terminal G of the intron. The function of the bulged nucleotide would then be to correctly place A868 for its interaction with the ribose moiety of the free or 3′-terminal G. The U870 and G870 mutants would be incapable of positioning A868 since they lack the requisite C_4–NH_2 group, resulting in a defective interaction with guanosine as reflected in the elevated K_m. The lack of site-specific hydrolysis in the mutants may also be due to their inability to position A868, for its interaction with the 3′-G may be required to facilitate hydrolysis at this splice site.

Finally, as suggested by the [Mg^{2+}] dependence of the mutants, the function of the bulged residue may be structural, helping dock the guanosine in the active site, either by a contribution to the overall conformation of the G-site or by a stacking interaction with the cofactor. Although the sensitivity of the mutants to streptomycin as well as the modest effect on V_{max} argues against gross distortions of the G-site, our data do not rule out either intramolecular interactions that appropriately configure the G-site, or a stacking interaction between the bulged residue and the cofactor. Interestingly, two H-bonds and a stacking interaction have been demonstrated between RNase T1 and guanine (Heinemann & Saenger, 1982).

Irrespective of the mechanism for promoting interaction of the ribozyme with guanosine, phenotypic suppression of the K_m phenotype by high pH (Figure 6) may help in defining the functional groups of the bulged residue. An increase in pH induces tautomeric changes that drive U and G into the enol form, causing U and G to simulate C and A (Saenger, 1984; Figure 2). This observation together with the common features of A and C residues suggests N_3 and/or C_4–NH_2 of the bulged C in group IA introns and N_1 and/or C_6–NH_2 of the bulged A in group IB introns as the functional groups in these phylogenetically conserved bulged residues.

Acknowledgments

We thank all members of our laboratory, especially P. Scott Chandry, for useful discussions. We thankfully acknowledge Jack Szostak and Rachel Green for providing 2-aminopurine and 2,6-diaminopurine, Francois Michel for many useful discussions, and Michael Yarus for sharing results prior to publication. We appreciate the efforts of Jonathan Clyman and Tim Coetzee in reviewing the manuscript and expert manuscript preparation by Carolyn Wieland and Maryellen Carl.

References

Ahsen, von, U., & Schroeder, R. (1990) *Nature 346*, 801.
Bartlet, J. A., Gaillard, R. K., Jr., & Joklik, W. K. (1986) *Biotechniques 4*, 308.
Bass, B. L., & Cech, T. R. (1984) *Nature 308*, 820–826.
Bass, B. L., & Cech, T. R. (1986) *Biochemistry 25*, 4473–4477.
Belfort, M., Moelleken, A., Maley, G. F., & Maley, F. (1983) *J. Biol. Chem. 258*, 2045–2501.
Belfort, M., Chandry, P. S., & Pedersen-Lane, J. (1987) *Cold Spring Harbor Symp. Quant. Biol. 52*, 181–192.
Burke, J. M., Belfort, M., Cech, T. R., Davies, R. W., Schweyen, R. J., Shub, D. A., Szostak, J. W., & Tabak, H. F. (1987) *Nucleic Acids Res. 15*, 7217–7221.
Burke, J. M., Esherik, J. S., Burfeind, W. R., & King, J. (1990) *Nature 344*, 80–82.
Cech, T. R. (1987) *Science 236*, 1532–1539.
Cech, T. R. (1988) *Gene 73*, 259–271.
Cech, T. R. (1990) *Annu. Rev. Biochem. 59*, 543–568.
Chandry, P. S., & Belfort, M. (1987) *Genes Dev. 1*, 1028–1037.
Christiansen, J., Douthwaite, S. R., Christensen, A., & Garrett, R. A. (1985) *EMBO J. 4*, 1019–1024.
Couture, S., Ellington, A. D., Gerber, A. S., Cherry, J. M., Doudna, J. A., Green, R., Hanna, M., Pace, U., Rajagopal, J., & Szostak, J. W. (1990) *J. Mol. Biol. 215*, 345–358.
Davies, R. W., Waring, R. B., Ray, J. A., Brown, T. A., & Scazzocchio, C. (1982) *Nature 300*, 719–724.
Ehrenman, K., Schroeder, R., Chandry, P. S., Hall, D. H., & Belfort, M. (1989) *Nucleic Acids Res. 17*, 9147–9163.
Hall, D. H., Povinelli, C. M., Ehrenman, K., Pedersen-Lane, J., Chu, F., & Belfort, M. (1987) *Cell 48*, 63–71.
Heinemann, U., & Saenger, W. (1982) *Nature 299*, 27–31.
Hicke, B. J., Christian, E. L., & Yarus, M. (1989) *EMBO J. 8*, 3843–3851.
Inoue, T., Sullivan, F. X., & Cech, T. R. (1985) *Cell 43*, 431–437.
Inoue, T., Sullivan, F. X., & Cech, T. R. (1986) *J. Mol. Biol. 189*, 143–165.
Kay, P. S., Menzel, P., & Inoue, T. (1988) *EMBO J. 7*, 3531–3537.
Kim, S.-H., & Cech, T. R. (1987) *Proc. Natl. Acad. Sci. U.S.A. 84*, 8788–8792.
Kunkel, T. A., Roberts, J. D., & Zakour, R. A. (1987) *Methods Enzymol. 154*, 367–383.
McSwiggen, J. A., & Cech, T. R. (1989) *Science 244*, 679–683.

Michel, F., & Westhof, E. (1990) *J. Mol. Biol. 216*, 585-610.
Michel, F., Jacquier, A., & Dujon, B. (1982) *Biochimie 64*, 867-881.
Michel, F., Hanna, M., Green, R., Bartel, D. P., & Szostak, J. W. (1989) *Nature 342*, 391-395.
Michel, F., Netter, P., Xu, M.-Q., & Shub, D. (1990) *Genes Dev. 4*, 777-788.
Noller, H. F., Asire, M., Barta, A., Douthwaite, S., Goldstein, T., Gutell, R., Moazed, D., Normancy, J., Prince, J. B., Stern, S., Triman, K., van Stock, B., Wheaton, V., Weiser, B., & Woese, C. R. (1986) in *Structure, Function and Genetics of Ribosomes* (Hardesty, B., & Kramer, G., Eds.) pp 143-163, Springer-Verlag, New York.
Parker, R., Siliciano, P. G., & Guthrie, C. (1987) *Cell 49*, 229-239.
Peebles, C. L., Perlman, P. S., Mecklenburg, K. L., Petrillo, M. L., Tabor, J. H., Jarrell, K. A., & Cheng, H.-L. (1986) *Cell 44*, 213-223.
Roy, S., Delling, U., Chen, C.-H., Rosen, C. A., & Sonenberg, N. (1990) *Genes Dev. 4*, 1365-1373.
Saenger, W. (1984) *Principles of Nucleic Acid Structure*, p 114, Springer-Verlag, New York.
Salvo, J. L. G., Coetzee, T., & Belfort, M. (1990) *J. Mol. Biol. 211*, 537-549.
Vieira, J., & Messing, J. (1987) *Methods Enzymol. 153*, 3-11.
Walstrum, S. A., & Uhlenbeck, O. C. (1990) *Biochemistry 29*, 10573-10576.
White, S. A., & Draper, D. E. (1989) *Biochemistry 28*, 1892-1897.
Williamson, C. L., Desai, N. M., & Burke, J. M. (1989) *Nucleic Acids Res. 17*, 675-689.
Wu, H.-N., & Uhlenbeck, O. C., (1987) *Biochemistry 26*, 8221-8227.
Yarus, M. (1988) *Science 240*, 1751-1758.
Zaug, A. J., Kent, J. R., & Cech, T. R. (1984) *Science 224*, 574-578.
Zaug, A. J., Kent, J. R., & Cech, T. R. (1985) *Biochemistry 24*, 6211-6218.

On the Structure of Platelet-Derived Growth Factor AA: C-Terminal Processing, Epitopes, and Characterization of Cysteine Residues†

Monika Jaumann, Viviane Hoppe, Dieter Tatje, Wolfram Eichner, and Jürgen Hoppe*
Physiologisch-Chemisches Institut der Universität Würzburg, Biozentrum, Am Hubland, D-8700 Würzburg, FRG
Received July 31, 1990; Revised Manuscript Received December 12, 1990

ABSTRACT: The complete amino acid sequence analysis of the "short" form of rPDGF-AA expressed in baby hamster kidney cells revealed the absence of posttranslationally modified amino acid. Approximately 50% of the proteins were shortened by two to three amino acid residues at the C-terminus. Trypsin treatment of BHK rPDGF-AA lead to the identification of two internal epitopes that correspond to the two previously described domains in rPDGF-BB [Vogel, S., & Hoppe, J. (1989) *Biochemistry 28*, 2961-2966]. Cysteine residues at positions 37, 46, 47, and 93, respectively, were converted by site-directed mutagenesis into serine residues, and the monomeric proteins were prepared through expression in *Escherichia coli*. None of the mutant proteins was able to dimerize, but all of them exhibited to various extents a reversible conformational change which may reflect an intermediate prefolded monomer. An intramolecular disulfide bridge between Cys-10 and Cys-91/93 was identified in these monomers. From a mixture of the mutant proteins 37 and 46, an active dimer was reconstituted, suggesting an intermolecular cysteine bridge between these two residues.

Platelet-derived growth factor (PDGF)[1] is a major mitogen in serum which promotes the proliferation of fibroblasts and smooth muscle cells in vitro (Heldin & Westermark, 1984; Deuel et al., 1985; Ross et al., 1986). The existence of two homologous PDGF chains termed A and B gives rise to the formation of three different dimeric forms: AA, AB, and BB. All these dimeric forms exist in nature with variable abundance (Waterfield et al., 1983; Doolittle et al., 1983; Betsholtz et al., 1986; Heldin et al., 1986; Hammacher et al., 1988; Bowen-Pope et al., 1989; Stroobant & Waterfield, 1984). For example, PDGF-AB is the predominant form in human platelet, whereas in porcine platelet extracts only the BB type was detected (Stroobant & Waterfield, 1984). PDGF-AA is more efficiently secreted from a variety of tumor cell lines (Heldin et al., 1986) while PDGF-BB, though expressed in significant quantities, remains membrane-associated in these cells (Robbins et al., 1985).

PDGF-AA may be synthesized in two different forms by means of a different splicing mechanism (Betsholtz et al., 1986; Hoppe et al., 1987; Rorsman et al., 1988; Bonthron et al., 1988). The two forms differ in their C-terminus (short and long form). Proteolytic processing of any of the two forms at the C-terminus like in PDGF-BB (Waterfield et al., 1983) would lead to identical termini. So far, there are no protein chemical data describing the C-terminal ending of PDGF-AA. Furthermore, the PDGF-A sequence contains a N-glycosylation consensus sequence. In light of the observation that rPDGF-AA from BHK cells (Eichner et al., 1989) exhibits some size heterogeneity, we have performed a complete protein sequence analysis showing that this heterogeneity arises from the partial cleavage of the two C-terminal residues.

The A and B forms are approximately 60% homologous, and the highest similarity is found in the center of the molecule comprising the eight cysteine residues (Betsholtz et al., 1986). One has therefore to assume a closely related tertiary structure.

† This work was supported by Grant SFB 176-A 10 from the Deutsche Forschungsgemeinschaft.
* Correspondence should be addressed to this author.

[1] Abbreviations: BHK, baby hamster kidney; SDS, sodium dodecyl sulfate.

0006-2960/91/0430-3303$02.50/0